Description of Bound Reactive Dynamics within the Approximate Quantum Trajectory Framework†

Sophya Garashchuk*

Department of Chemistry and Biochemistry, University of South Carolina, Columbia, South Carolina 29208

Received: December 15, 2008; Revised Manuscript Received: February 20, 2009

The quantum trajectory framework incorporates quantum effects on dynamics through the quantum potential acting on a trajectory ensemble in addition to the classical potential. A global quadratic approximation to the quantum potential makes the method practical in many dimensions and captures dominant quantum effects in semiclassical systems. In this paper the approach is further developed to describe the "double well" dynamics—a prototype of the proton transfer reactions—which exhibits the "hard" quantum effect of tunneling. Accurate description is achieved by combining the approximate quantum trajectory dynamics with the population amplitudes in the reactant and product wells. The quantum trajectory dynamics is defined by the asymptotic classical potentials. The population amplitudes represented in a small basis describe transfer between the wells. The method is exact if the reactant/product potentials are quadratic and the basis size is sufficiently large. In the semiclassical regime the trajectory dynamics is approximate and the basis size can be as small as two functions. The approach is fully compatible with the trajectory description of multidimensional systems capturing quantum tunneling along the reactive coordinate and zero-point energy flow among all degrees of freedom.

I. Introduction

Quantum-mechanical (QM) effects in molecular dynamics—zero-point energy, tunneling, and nonadiabatic dynamics—are essential for accurate description and understanding of reactions in complex molecular systems. The proton transfer reactions in condensed phase are of special practical importance,[1−4] yet they cannot be modeled accurately in full dimension because of (a) the exponential scaling of the conventional methods of solving the Schrödinger equation (SE)[5] with the system size, and because of (b) the long-time scale of relevant dynamics.[6] While there are multidimensional quantum approaches based on basis set contraction and[7−9] coherent state representations[10,11] as well as mixed quantum/classical strategies,[12−18] a trajectory representation of large molecular systems has special appeal. (i) Initial conditions can be sampled with the Monte Carlo techniques circumventing exponential scaling of exact QM. (ii) All degrees of freedom (DoFs) can be treated on equal footing avoiding quantum/classical separation issues.[19] (iii) The trajectory description of heavy particles (such as nuclei) is often more appropriate than the grid or basis set representations, because the wave function is highly oscillatory in $\hbar \to 0$ limit. (iv) Classical equations of motion are cheap to solve: methods of molecular mechanics[20] based on classical trajectories are routinely applied to high-dimensional systems of hundreds of atoms. The challenge for the trajectory dynamics methods is incorporation of the dominant QM effects caused by the wave function localization.[21,22] Therefore, it is logical to consider representing the wave function in terms of a trajectory ensemble rather than in terms of independent trajectories as common in semiclassical methods.[23−25]

Semiclassical dynamics with the approximate quantum potential (AQP) is based on the de Broglie−Bohm formulation[26] of the time-dependent SE. Here and below, the term "semiclassical" is used not in a sense of formal expansions with respect to small parameter $\hbar$, but refers to systems for which classical treatment gives reasonable qualitative description of their properties and the quantum corrections are small yet important. In the de Broglie−Bohm formulation the wave function, represented in terms of the real amplitude $A(x,t)$ and phase $S(x,t)$,

$$\psi(x,t) = A(x,t)\exp\left(\frac{i}{\hbar}S(x,t)\right) \tag{1}$$

is discretized in coordinate space in terms of the quantum trajectories (QTs) with positions x and momenta p,

$$p(x,t) = \nabla S(x,t) \tag{2}$$

Unlike trajectories of the conventional classical/semiclassical methods, the QTs evolve according to Newton's laws of motion in the presence of the additional *quantum potential*.

$$U = -\frac{\hbar^2}{2m}\frac{\nabla^2 A(x,t)}{A(x,t)} \tag{3}$$

Here m is the mass of a particle. For clarity the formalism is given for one Cartesian dimension suppressing arguments of functions if unambiguous. Generalizations can be found in ref 27.

The time evolution of the wave function density, $\rho(x,t) = A^2(x,t)$, along the trajectory, that is, in the Lagrangian frame of reference, is given by

† Part of the "George C. Schatz Festschrift".

* To whom correspondence should be addressed. E-mail: sgarashc@mail.chem.sc.edu.

10.1021/jp8110869 CCC: $40.75
Published on Web 03/16/2009

$$\frac{\mathrm{d}}{\mathrm{d}t}\rho(x,t) = \left(\frac{\partial}{\partial t} + \frac{p}{m}\frac{\partial}{\partial x}\right)\rho(x,t) = -\nabla p\ \rho(x,t) \qquad (4)$$

From eq 4 it follows that for closed systems the probability of finding a particle in a volume element associated with each QT—the trajectory "weight"—remains constant in time,[28]

$$w(x) = \rho(x,t)\,\delta x(t), \quad \frac{\mathrm{d}w}{\mathrm{d}t} = 0 \qquad (5)$$

Therefore, the QT description, which is equivalent to the time-dependent SE, provides an ideally compact coordinate space representation of $\psi(x,t)$. The quantum behavior is compressed into a *single nonlocal* quantity—the quantum potential given by eq 3.

QTs provide an intuitive visualization of the wave function density evolution,[29] and the formalism has been extended to nonadiabatic dynamics,[30−32] to the phase-space representations, to the density matrix approaches,[33−40] and to the arbitrary coordinate systems.[27] Several high-dimensional exact QT applications have been reported,[41,42] but for general, even low-dimensional systems the exact implementation is impractical because of the singularities in the quantum potential.[43−46] This motivated some interesting alternative implementations based on the Taylor expansion of the equations of motion,[47,48] on the bipolar decomposition of wave functions,[49,50] and on the complex QTs.[51]

We use the QT formalism as a basis for a *well-defined semiclassical* propagation method using a single approximation to the quantum potential.[52] The classical limit can be defined as the AQP being zero. When the AQP is determined with high accuracy, the formulation approaches full QM limit. We are interested in the intermediate regime when the AQP is simple enough to be determined globally (in other words, it is determined for all trajectories at once, without analyzing the vicinity of each trajectory separately), making it efficient and practical in many dimensions, and at the same time is accurate enough to describe leading quantum effects in semiclassical regime appropriate for dynamics of nuclei.

The central idea is to determine the AQP from the *global* least-squares fit to the nonclassical component of the momentum operator,

$$r(x,t) = \frac{\nabla A(x,t)}{A(x,t)} \approx \vec{c}\cdot\vec{f}(x) \qquad (6)$$

at each time t in a small basis $\vec{f}(x)$. The physical motivation for focusing on $r(x,t)$ is that it complements the classical momentum $p(x,t)$ to give a full description of the quantum trajectory ensemble and that its effect on dynamics vanishes as $\hbar \to 0$. The least-squares fit procedure is reducible to the system of linear equations of the size of the basis. The matrix elements can be found from a single summation over trajectory weights given by eq 5, which eliminates numerical difficulties associated with small $A(x,t)$ in eq 6, because $r(x,t)$ is formally multiplied by $A^2(x,t)$ in computation of average quantities. The energy is strictly conserved because the least-squares fit of r weighted by the wave function density is equivalent to the variation of the average AQP[53] with respect to the fitting parameters. The linear basis gives exact Gaussian wavepacket dynamics and describes the dominant QM effects in general systems.[54] In principle, the method can be taken to the exact QM limit using subspaces[54] or complete bases,[55] though it might be expensive if the interference effects on dynamics are large. The methodology has been also extended to nonadiabatic systems using the complex population amplitudes on multiple electronic surfaces.[31,56] Most importantly, the approach is cheap with essentially linear scaling of the numerical effort with the system size.

The AQP method has been applied to several triatomic reactive systems in gas phase,[54,56] where the leading quantum effects were reproduced on the reaction time scale of a few molecular vibrations. Dynamics studies of complex molecular systems, however, may require propagation for picoseconds. To this end, the original approach has been extended to give stable description of ZPE in anharmonic degrees of freedom.[57] The key was to treat dynamics of classical and nonclassical components of the momentum operator given by eqs 2 and 6, respectively, on equal footing which balances errors,

$$m\left(\frac{\mathrm{d}p}{\mathrm{d}t} + \nabla V\right) = \left(r + \frac{\nabla}{2}\right)\frac{\partial r}{\partial x}$$
$$-m\frac{\mathrm{d}r}{\mathrm{d}t} = \left(r + \frac{\nabla}{2}\right)\frac{\partial p}{\partial x} \qquad (7)$$

and to compensate for the truncation of equations of motion on the level of equations. Model calculations were performed for an unbound reactive coordinate in the presence of up to 40 Morse oscillators. The wavepacket coherence and associated with it "quantum" energy $\langle U\rangle$, which is one-half of ZPE for the harmonic oscillator eigenstates, were reproduced for hundreds of oscillation periods. In the remainder of the paper we address the outstanding methodological challenge: description of bound reactive dynamics compatible with the trajectory description of the high-dimensional anharmonic bath.

II. Bound Dynamics with Tunneling

In general, semiclassical methods are not expected to accurately describe "hard" quantum effects, such as tunneling and interference. In this regime, the exact QT dynamics is numerically unstable, because the exact quantum potential of eq 3 is singular due to the nodes of $\psi(x,t)$. The AQP trajectories are stable, but quantum forces quickly become inaccurate, trajectories decohere and dynamics becomes essentially classical. For an initially localized wave function evolving in the double well potential—a prototype model of the proton transfer in condensed phase—the key dynamics feature is tunneling between the "reactant" and "product" wells. To capture this "hard" quantum effect in the trajectory framework, we represent the wave function as

$$\psi(x,t) = \chi_1(x,t)\,\phi_1(x,t) + \chi_2(x,t)\,\phi_2(x,t) \qquad (8)$$

Wave functions ϕ_1 and ϕ_2 evolve independently of each other in the asymptotic potentials of reactants and products V_1 and V_2, respectively, according to the SE

$$i\hbar\frac{\partial\phi_j}{\partial t} = \frac{\hbar^2}{2m}\frac{\partial^2\phi_j}{\partial x^2} + V_j\phi_j, \quad j = 1,2 \qquad (9)$$

For chemical systems, asymptotic dynamics can be sufficiently simple to be accomplished semiclassically with two ensembles of the AQP trajectories. Below the superscripts will label quantities associated with trajectories in these two ensembles.

The tunneling or population transfer between the two wells under the influence of the full potential V is accomplished through the complex amplitudes χ_1 and χ_2. These two functions will be represented in a basis $\vec{f}$ of N_b polynomials, for example in the Taylor basis $\vec{f} = (1,x,x^2,...)$:

$$\chi_1 = \sum_{n=1,N_b} c_n(t)x^{n-1}, \quad \chi_2 = \sum_{n=1,N_b} c_{n+N_b}(t)x^{n-1} \tag{10}$$

Multiplication of the SE for the function ψ given by eq 8 by the components of the total basis of ψ,

$$\vec{F} = (f_1\phi_1, ..., f_{N_b}\phi_1, f_1\phi_2, ..., f_{N_b}\phi_2) \tag{11}$$

and integration over x gives a linear system of differential equations for the basis coefficients $\vec{c}$,

$$i\hbar\mathbf{S}\dot{\vec{c}} = \mathbf{H}\vec{c} \tag{12}$$

Equation 9 has been used to obtain the last result. Matrix **S**,

$$\mathbf{S} = \langle \vec{F} \otimes \vec{F} \rangle \tag{13}$$

is the time-dependent overlap matrix of the size $2N_b$. The right-hand-side of eq 12 is a "partial" Hamiltonian matrix **H**,

$$\mathbf{H} = \langle \vec{F} \otimes (\vec{K} + \vec{\Pi}) \rangle \tag{14}$$

containing the derivatives of χ_i as well as the potential energy terms. The matrix is constructed as the outer product of the basis function vector $\vec{F}$ given by eq 11 and the vector $\vec{K} + \vec{\Pi}$ whose elements are given by

$$K_i = -\frac{\hbar^2}{2m}\left(\frac{\partial^2 f_i}{\partial x^2}\phi_j + 2\frac{\partial f_i}{\partial x}\frac{\partial \phi_j}{\partial x}\right) \tag{15}$$

$$\Pi_i = (V - V_j)F_i \tag{16}$$

where $j = 1$ for $1 \le i \le N_b$ and $j = 2$ for $N_b + 1 \le i \le 2N_b$.

In the AQP implementation, the integrals in the diagonal blocks of the matrices can be readily expressed as sums over trajectory weights,

$$\int |\phi_j(x,t)^2| o(x)\, dx = \sum_k o(x_k^{(j)}) w_k^{(j)} \tag{17}$$

k indexing the trajectories. In the minimal basis set, $N_b = 1$, related to the two state representation of the system[58] there are no kinetic energy terms. The AQP dynamics is exact for Gaussian wave functions governed by the harmonic asymptotic potentials $V_{1,2}$. Functions $\phi_{1,2}$ and their derivatives are known analytically in this case, and the whole approach becomes exact for a sufficiently large basis for $\chi_{1,2}$. In the semiclassical regime in order to use the minimal basis for χ, we can define anharmonic $V_{1,2}$ and use the approximate evolution of r and p given by linearized and stabilized eq 7.[57] Then, the derivatives of ϕ_j at the trajectory positions are

$$\left.\frac{\partial \phi_j}{\partial x}\right|_{x_s = x_k^{(j)}} = (r_k^{(j)} + ip_k^{(j)})\phi_j \tag{18}$$

In the off-diagonal matrix elements, $\langle \phi_1 | o(\hat{x}) | \phi_2 \rangle$ we use the linearization parameters of r and p, already available from the AQP dynamics, for evaluation of ϕ_2 at the positions $x_k^{(1)}$ of the first trajectory set and vice verse. The mixed-type integrals are evaluated in a symmetrized fashion,

$$2\langle \phi_1 | o(\hat{x}) | \phi_2 \rangle = \sum_{j=1,2} \sum_k o(x_k^{(j)})\, w_k^{(j)} z(x_k^{(j)}) \tag{19}$$

The ratio of the wave functions, $z(x) = \phi_2(x)/\phi_1(x)$, is found from the linearizations of $r^{(j)}$ and $p^{(j)}$ as well.

Note that the overlap matrix **S** is Hermitian and, generally, is time-dependent. The Hamiltonian matrix **H** is complex and, generally, is nonsymmetric. Conservation of the total wave function normalization,

$$N = \vec{c}^{\dagger}\mathbf{S}\vec{c} \tag{20}$$

can be expressed as

$$\vec{c}^{\dagger}\left(i\frac{d}{dt}\mathbf{S} + \mathbf{H} - \mathbf{H}^{\dagger}\right)\vec{c} = 0 \tag{21}$$

Equation 21 is not necessarily satisfied in the course of the approximate dynamics.

III. Test Applications and Discussion

The first numerical illustration is performed for a total potential consisting of two harmonic wells coupled by a switching function,

$$V = \frac{1}{2}(V_1(1 - \tanh \kappa x) + V_2(1 + \tanh \kappa x)) \tag{22}$$

The asymptotic potentials are

$$V_j = (x - x_0^{(j)})^2/2$$

In atomic units, the parameter values are $k = 4$, $x_0^{(1)} = -(2)^{1/2}$, $x_0^{(2)} = (2)^{1/2}$. The potential is shown on Figure 1a. The initial wave function is a Gaussian wavepacket localized in the left well,

$$\phi_1(x,0) = \left(\frac{2\gamma}{\pi}\right)^{1/4} \exp(-\gamma(x - q_0^{(1)})^2 + ip_0^{(1)}) \tag{23}$$

The initial "image" Gaussian ϕ_2 has the same form as ϕ_1 with $q_0^{(2)} = -q_0^{(1)}$ and $p_0^{(2)} = -p_0^{(1)}$. The corresponding population functions are $\chi_1(x,0) = 1$ and $\chi_2(x,0) = 0$. In general, one can use more compact basis for χ if ϕ_2 is chosen such that it has large overlap with the barrier region at times when ϕ_1 has significant overlap with the barrier.

Figure 1 shows quantities relevant to the initial wave function $\psi(x,0) = \phi_1(x,0)$ which is an eigenstate of V_1 and centered in the left well, $q_0^{(1)} = x_0^{(1)}$ on panels a and b. Panels c and d correspond to the displaced $\psi(x,0)$ with $q_0^{(1)} = x_0^{(1)} - 0.4a_0$. The particle has a

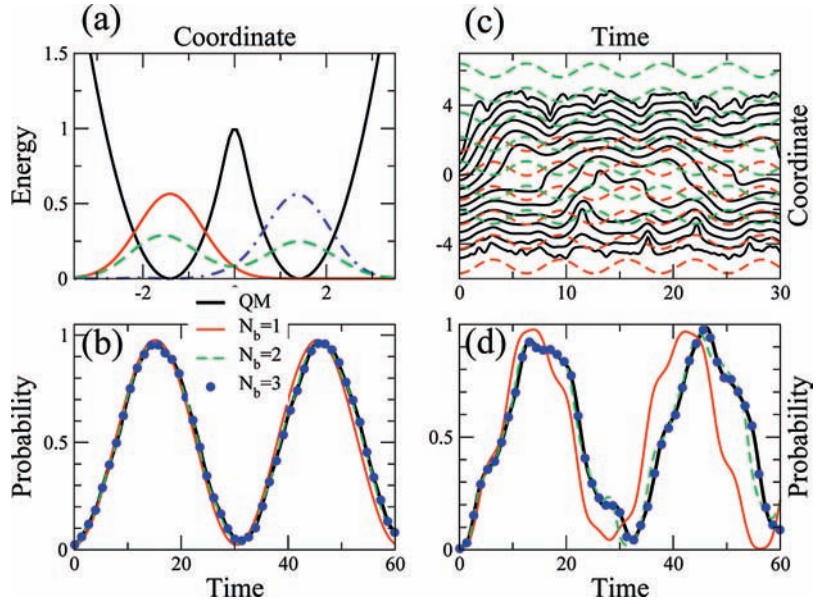

Figure 1. Dynamics in the double well potential with quadratic walls. (a) Potential (black solid line) and QM wave function density, $|\psi(x,t)|^2$, at $t = 0$ (red solid), $t = 7.5$ (green dash) and $t = 15$ (blue dot-dash). (c) QM trajectories (solid black) and two sets of the AQP trajectories of the new formulation (red and green dash). (b and d) QM and AQP probabilities of a system to be in the right well. On panels a and b $\psi(x,0)$ is initially centered at the bottom of the left well, $q_0^{(1)} = x_0^{(1)}$; on panels c and d $\psi(x,0)$ is initially displaced.

unit mass. Functions $\phi_{1,2}$ are coherent wavepackets with the width parameter $\gamma = 0.5$ and zero initial momenta, $p_0^{(j)} = 0$. For eigenstates the classical potential is compensated up to a constant by the quantum potential. Thus, there is no force acting on the trajectories evolving under the potentials $V_{1,2}$ and they remain stationary. The population of the right well,

$$P(t) = \int_0^\infty |\psi(x,t)|^2 \, dx \tag{24}$$

as a function of time is shown on panel b. We see that the minimal basis,

$$\psi(x,t) = \sum_j c_j(t) \, \phi_j(x,t) \tag{25}$$

gives a small time-shift in $P(t)$ compared to QM result, whereas results for the linear basis track the quantum behavior very closely.

On panel c the trajectories for the initially displaced wave function are shown. The exact QTs for the full potential V are compared with the trajectories evolving in the asymptotic potentials. Note the complicated and unstable (!) behavior associated with V as the wave function is transferred between the wells in "installments" which interfere constructively. The "asymptotic" trajectories follow the basic coherent oscillatory motion. $P(t)$ on panel d shows irregular oscillations, which are not well captured in the minimal basis; linear basis already gives very good agreement and quadratic basis gives essentially exact result.

The next example involves strongly anharmonic double well, which is the reactive coordinate potential in the proton transfer model of Topaler and Makri[59] that became the benchmark for approximate and semiclassical methods. With the particle mass rescaled to $m = 1$ the potential is

$$V = 14x^4 - 20x^2 + 50/7 \tag{26}$$

The parameters of the initial Gaussian wavepacket given by eq 23 are chosen so that $\psi(x,0)$ resembles the part of the ground-state localized in the left well: $\gamma = 4.47$, $x_0 = -0.77$, and $p_0 = 0$. The parameters of the asymptotic potential V_1 are chosen to minimize its deviation from the full potential, $\langle (V - V_1)^2 \rangle$, weighted by the initial wave function density $|\psi(x,0)|^2$. The product asymptotic potential V_2 is a reflection of V_1, $V_2(x) = V_1(-x)$. We consider two asymptotic potentials: (A) the quadratic potential,

$$V_1^{\mathrm{A}} = \frac{k(x + q_0)^2}{2}$$

and (B) the Morse oscillator,

$$V_1^{\mathrm{B}} = D(\exp(-z(x + q_0)) - 1)^2$$

The parameters are $k = 34.500$, $q_0 = 0.741$, and $D = 28.204$, $z = 1.114$, $q_0 = 0.836$.

Figure 2a shows the full potential and its asymptotic approximations, V_1^{A} and V_1^{B}, as well as the initial wave function density in arbitrary scale. The initial energy of the wavepacket constitutes 59% of the barrier height. The probability for the particle to be in the right well given by eq 24 obtained with the asymptotic dynamics in the quadratic potential is shown on Figure 2b. Unlike our first example where V (eq 22) has quadratic potentials as exact asymptotes, to capture the QM behavior for the quartic potential of eq 26 we need the basis of $\chi_{1,2}$ at least as large as four functions, $N_b = 4$, mostly to account for the effects of the steep wall on dynamics in the well. The advantage of the quadratic functional form for V_1^{A} is that the trajectory dynamics of the Gaussians $\phi_{1,2}$ and, consequently, evaluation of matrix elements are exact. Therefore, we have the exact QM limit of the new procedure.

The semiclassical description of the same system consists of the AQP dynamics in the asymptotic potential—the Morse

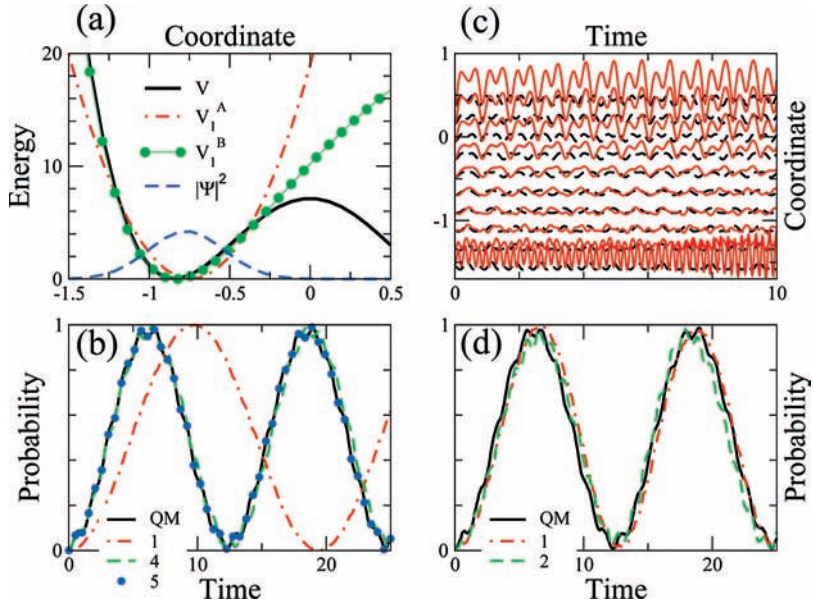

Figure 2. Dynamics in the double well potential with quartic walls. The oscillation period in the asymptotic well is approximately 1.4 atomic units. (a) Full potential V (solid line) and its quadratic V_1^A (dot-dash) and Morse V_1^B (circles) asymptotes. Initial wave function density, $|\psi(x,t)|^2$, in arbitrary units is also shown. (b and d) Probability of finding the particle in the product well as a function of time with dynamics under V_1^A (b) and V_1^B (d). Exact QM results and the trajectory results for several basis sizes, N_b, are labeled on the figure. (c) The approximate quantum trajectories describing ϕ_1 for V_1^A (dash) and for V_1^B (solid line).

oscillator of V_1^B, which is closer to the full potential in the well region than V_1^A, and a small basis for $\chi_{1,2}$. Dynamics under the influence of $V_{1,2}^B$ has most of the anharmonicity in the well built into the time-dependence of $\phi_{1,2}$ as illustrated in Figure 2d. Simple coordinate-independent prefactors ($N_b = 1$, eq 25) capture oscillations in the probabilities rather accurately. $N_b = 2$ gives agreement with the quantum result of about the same quality as $N_b = 1$. The AQP dynamics is accomplished as described in ref57 using the balanced time-evolution equations of p and r. The trajectories corresponding to ϕ_1 are shown on Figure 2c. Remarkably, for the center of the wavepacket the difference between dynamics with V_1^A and V_1^B is not dramatic: both show low amplitude oscillations. The large amplitude oscillations in positions of trajectories on the fringes of ϕ_1 are the result of the stabilization terms, without which trajectories decohere after $t = 5$. The difference in the quality of the minimal $N_b = 1$ description for the two asymptotic potentials, however, is qualitative. It should be also noted, that the total norm-conservation expressed by eq 21 is not guaranteed in the approximate implementation. In the case of $N_b = 1$, normalization given by eq 20 is conserved better than 1% at all times, and the mean deviation from $N = 1$ is 0.25%. For the basis with linear functions, $N_b = 2$, the maximum discrepancy in the total normalization is 14% and the mean deviation is 4%. The probabilities shown on Figure 2 are normalized, though this operation does not make noticeable changes. Solution of eq 12 for a larger basis size with the AQP dynamics is unstable. Since the error in normalization with $N_b = 1$ is very small we conclude that the approximate dynamics itself, which *does not depend* on the basis size of χ is rather accurate. Larger error for $N_b = 2$ and instability for $N_b \geq 3$ can be explained by the errors in the matrix element evaluations given by eqs 18 and 19 amplified in the higher moments of larger basis sets. In general, we believe a combination of small basis set for χ with the stabilized AQP dynamics is appropriate for "semiclassical" systems. Nevertheless, the normalization conservation can be, in principle, included into fitting of r and p in the AQP dynamics, providing a connection between the basis set and trajectory parts of the total wave function. This issue as well as multidimensional applications will be investigated in the future.

IV. Conclusions

We have presented a new approach of describing tunneling regime of the "double well" within the framework of approximate quantum trajectories. The central idea is the semiclassical treatment of the semiclassical part of the problem—description of ZPE using the approximate quantum trajectories to evolve wavepackets in the asymptotic potentials of reactants and products consisting of single wells. The "hard" quantum effect of tunneling between the wells is described with the small basis set of complex amplitudes. The approach is somewhat similar to the description of another "hard" QM effects—nonadiabatic dynamics and interference—developed earlier.[32,60] The QM limit of the new approach is well-defined and can be reached in a straightforward manner by increasing the basis set size combined with the Gaussian wavepacket evolution, though it might become expensive for dynamics with strong interference effects. In the semiclassical regime, the minimal basis combined with the stabilized AQP in the anharmonic asymptotic potentials gives a fairly accurate description of the probability oscillations between the wells. The advantage of the mixed formulation is that it is fully integrated with the trajectory description of multidimensional systems. Thus, it will be practical for high dimensional problems, such as proton transfer reaction in condensed phase, where the basis can be used for just the reaction coordinate and QM tunneling is expected to be quenched by the interaction with the bath DoFs. This is the direction of our current research.

References and Notes

(1) Dekker, C.; Ratner, M. A. *Phys. World* **2001**, *14*, 29.
(2) Lear, J. D.; Wasserman, Z. R.; DeGrado, W. F. *Science* **1988**, *240*, 1177.
(3) Cha, Y.; Murray, C. J.; Klinman, J. P. *Science* **1989**, *243*, 1325.
(4) Knapp, M. J.; Klinman, J. P. *Eur. J. Biochem.* **2002**, *269*, 3113.
(5) Light, J. C.; Carrington, T., Jr. *Adv. Chem. Phys.* **2000**, *114*, 263.

(6) Ussing, B. R.; Hang, C.; Singleton, D. A. *J. Am. Chem. Soc.* **2006**, *128*, 7594.
(7) Wang, H. B.; Thoss, M. *J. Chem. Phys.* **2003a**, *119*, 1289.
(8) Meyer, H. D.; Worth, G. A. *Theor. Chem. Acc.* **2003**, *109*, 251.
(9) Wang, H. B.; Thoss, M. *J. Chem. Phys.* **2003b**, *119*, 1289.
(10) Shalashilin, D. V.; Child, M. S. *J. Chem. Phys.* **2004**, *121*, 3563.
(11) Wu, Y. H.; Batista, V. S. *J. Chem. Phys.* **2006**, *124*, 224305.
(12) Ben-Nun, M.; Q., J; Martinez, T. J. *J. Chem. Phys.* **2001**, *104*, 5161.
(13) Kim, S. Y.; Hammes-Schiffer, S. *J. Chem. Phys.* **2006**, *124*, 244102.
(14) Prezhdo, O.; Kisil, V. V. *Phys. Rev. A* **1997**, *56*, 162.
(15) Hone, T. D.; Izvekov, S.; Voth, G. A. *J. Chem. Phys.* **2005**, *122*, 054105.
(16) Gao, J.; Truhlar, D. G. *Annu. Rev. Phys. Chem.* **2002**, *53*, 467.
(17) Náray-Szabó, G. Warshel, A., Eds. *Computational Approaches to Biochemical Reactivity*; Understanding Chemical Reactivity, Vol. 19; Kluwer Academic Publishers: Dordrecht, The Netherlands, 1997.
(18) Gindensperger, E.; Meier, C.; Beswick, J. A. *J. Chem. Phys.* **2000**, *113*, 9369.
(19) Prezhdo, O. V.; Brooksby, C. *Phys. Rev. Lett.* **2001**, *86*, 3215.
(20) Karplus, M.; Sharma, R. D.; Porter, R. N. *J. Chem. Phys.* **1964**, *40*, 2033.
(21) McCormack, D. A.; Lim, K. F. *J. Chem. Phys.* **1997**, *106*, 572.
(22) Guo, Y.; Thompson, D. L. *J. Chem. Phys.* **1996**, *104*, 576.
(23) Herman, M. F.; Kluk, E. *Chem. Phys.* **1984**, *91*, 27.
(24) Kay, K. G. *J. Chem. Phys.* **1994**, *100*, 4377.
(25) Miller, W. H. *J. Phys. Chem. A* **2001**, *105*, 2942.
(26) Bohm, D. *Phys. Rev.* **1952**, *85*, 166.
(27) Rassolov, V. A.; Garashchuk, S.; Schatz, G. C. *J. Phys. Chem. A* **2006**, *110*, 5530.
(28) Garashchuk, S.; Rassolov, V. A. *Chem. Phys. Lett.* **2002**, *364*, 562.
(29) Sanz, A. S.; Borondo, F.; Miret-Artes, S. *J. Phys. (Paris)* **2002**, *14*, 6109.
(30) Wyatt, R. E.; Lopreore, C. L.; Parlant, G. *J. Chem. Phys.* **2001**, *114*, 5113.
(31) Rassolov, V. A.; Garashchuk, S. *Phys. Rev. A* **2005**, *71*, 032511.
(32) Garashchuk, S.; Rassolov, V. A.; Schatz, G. C. *J. Chem. Phys.* **2005**, *123*, 174108.
(33) Burghardt, I.; Cederbaum, L. S. *J. Chem. Phys.* **2001**, *115*, 10303.
(34) Burghardt, I.; Cederbaum, L. S. *J. Chem. Phys.* **2001**, *115*, 10312.
(35) Burghardt, I.; Moller, K. B. *J. Chem. Phys.* **2002**, *117*, 7409.
(36) Maddox, J. B.; Bittner, E. R. *J. Phys. Chem. B* **2002**, *106*, 7981.
(37) Bittner, E. R.; Maddox, J. B.; Burghardt, I. *Int. J. Quantum Chem.* **2002**, *89*, 313.
(38) Donoso, A.; Martens, C. C. *Phys. Rev. Lett. 87* **2001**, *1*, 223202.
(39) Trahan, C. J.; Wyatt, R. E. *J. Chem. Phys.* **2003**, *119*, 7017.
(40) Donoso, A.; Martens, C. C. *J. Chem. Phys.* **2002**, *116*, 10598; URL http://link.aip.org/link/?JCP/116/10598/1.
(41) Wyatt, R. E.; Na, K. *Phys. Rev. E 65* **2002**, 0167021.
(42) Babyuk, D.; Wyatt, R. E. *J. Chem. Phys.* **2006**, *124*, 2141091.
(43) Bittner, E. R. *J. Chem. Phys.* **2000**, *112*, 9703.
(44) Wyatt, R. E.; Bittner, E. R. *J. Chem. Phys.* **2000**, *113*, 8898.
(45) Kendrick, B. K. *J. Chem. Phys.* **2003**, *119*, 5805.
(46) Wyatt, R. E. CNLS Workshop: Quantum and Semiclassical Molecular Dynamics of Nanostructures; Los Alamos National Laboratory, July 15–17, 2004.
(47) Trahan, C. J.; Hughes, K.; Wyatt, R. E. *J. Chem. Phys.* **2003**, *118*, 9911.
(48) Liu, J.; Makri, N. *J. Phys. Chem. A* **2004**, *108*, 5408.
(49) Poirier, B. *J. Chem. Phys.* **2004**, *121*, 4501.
(50) Park, K.; Poirier, B.; Parlant, G. *J. Chem. Phys.* **2008**, *129*, 194112;URL http://link.aip.org/link/?JCP/129/194112/1.
(51) Goldfarb, Y.; Degani, I.; Tannor, D. J. *J. Chem. Phys.* **2006**, *125*, 231103.
(52) Garashchuk, S.; Rassolov, V. A. *J. Chem. Phys.* **2003**, *118*, 2482.
(53) Garashchuk, S.; Rassolov, V. A. *J. Chem. Phys.* **2004**, *120*, 1181.
(54) Rassolov, V. A.; Garashchuk, S. *J. Chem. Phys.* **2004**, *120*, 6815.
(55) Garashchuk, S.; Rassolov, V. A. *Chem. Phys. Lett.* **2007**, *446*, 395.
(56) Garashchuk, S.; Rassolov, V. A.; Schatz, G. C. *J. Chem. Phys.* **2006**, *124*, 244307.
(57) Garashchuk, S.; Rassolov, V. A. *J. Chem. Phys.* **2008**, *129*, 024109.
(58) Landau, L. D.; Lifshitz, E. M., *Quantum Mechanics;* Butterworth-Heinemann: Oxford, UK, 1999.
(59) Makri, N. *J. Phys. Chem. A* **1998**, *102*, 4414.
(60) Garashchuk, S.; Rassolov, V. A. *J. Chem. Phys.* **2004**, *121*, 8711.

JP8110869